Lab on a Chip

PAPER

View Article Online
View Journal | View Issue

Bacterial chemotaxis on SlipChip†

Cite this: *Lab Chip*, 2014, **14**, 3074

Chaohua Shen,[ab] Peng Xu,[b] Zhou Huang,[b] Dongyang Cai,[b] Shuang-Jiang Liu*[b] and Wenbin Du*[b]

Received 18th February 2014,
Accepted 21st May 2014

DOI: 10.1039/c4lc00213j

www.rsc.org/loc

This paper describes a simple and reusable microfluidic SlipChip device for studying bacterial chemotaxis based on free interface diffusion. The device consists of two glass plates with reconfigurable microwells and ducts, which can set up 20 parallel chemotaxis units as duplicates. In each unit, three nanoliter microwells and connecting ducts were assembled for pipette loading of a chemoeffector solution, bacterial suspension, and 1X PBS buffer solution. By a simple slipping operation, three microwells were disconnected from other units and interconnected by the ducts, which allowed the formation of diffusion concentration gradients of the chemoeffector for inducing cell migration from the cell microwell towards the other two microwells. The migration of cells in the microwells was monitored and accurately counted to evaluate chemotaxis. Moreover, the migrated cells were easily collected by pipetting for further studies after a slip step to reconnect the chemoeffector microwells. The performance of the device was characterized by comparing chemotaxis of two *Escherichia coli* species, using aspartic acid as the attractant and nitrate sulfate as the repellent. It also enables the separation of bacterial species from a mixture, based on the difference of chemotactic abilities, and collection of the cells with strong chemotactic phenomena for further studies off the chip.

Introduction

Chemotaxis is an important behavior of biological cells that enables them to sense chemical gradients and direct their migration.[1–6] Many cells are guided by a chemotactic response towards favorable colonization sites or away from toxins. For example, chemokines play an important role in metastasis and angiogenesis;[7] autoimmune inflammatory disorders, such as atherosclerosis, are induced by pro-inflammatory cytokines;[8] *Helicobacter Pylori* is guided to the mucus lining of the human stomach,[9] resulting in increased rates of host infection; toluene-degrading *Pseudomonas putida* f1 moves towards environmental pollutants, which can be exploited for bioremediation.[10]

The study of chemotaxis relies on tools that generate and maintain chemical gradients and monitor the dynamic distribution of living cells. In recent years, microfluidic technologies have boosted the emergence of various powerful tools for analyzing numerous biological processes,[11–15] including the development of various devices for improving chemotaxis assays of bacterial and mammalian cells.[15–19] These microfluidic devices can be classified as flow-based methods and diffusion-based methods. The flow-based devices provide a well-controlled gradient with a stable laminar flow.[20] However, it is difficult to preserve cell autocrine/paracrine secretion in continuous flow systems, which may have impact on cell migration.[21] Chemotaxis of cells in flow is also affected by hydrodynamic shear stress.[22] On the other hand, diffusion-based methods provide a flow-free environment by introducing diffusive barriers, such as membranes,[23] self-assembled microspheres[24] or hydrogels,[25] to precisely control chemical diffusion. However, the fabrication and preparation of diffusion barriers remain technical obstacles which prevent these devices from being widely applied. In addition, current diffusion-based methods are generally not able to selectively harvest the cells of interest.

SlipChips are microfluidic devices which control multiplexed liquid experiments at nanoliter scales by slipping plates in close contact.[26–28] Recently, various interesting applications have been demonstrated, including protein crystallization,[29] polymerase chain reaction,[30,31] and immunoassay-based diagnostics.[27] In a device for protein crystallization screening based on free interface diffusion (FID),[29] controllable and variable diffusion concentration gradients were generated for optimizing protein crystal nucleation and growth.[29] Illuminated by this FID design and features, we described in this paper a simple microfluidic SlipChip device which was used to set up gradient-driven chemotaxis

[a] *Department of Chemistry, Renmin University of China, 100872 Beijing, China*
[b] *State Key Laboratory of Microbial Resources, Institute of Microbiology, Chinese Academy of Sciences, Beijing 100101, China. E-mail: wenbin@im.ac.cn, liusj@im.ac.cn*

† Electronic supplementary information (ESI) available: An optimized version of the AutoCAD design of the SlipChip device for performing four different chemotaxis experiments each with twenty duplicates was provided. DOI: 10.1039/c4lc00213j

experiments. The diffusion process in the chemotaxis experiment was initiated or terminated by slipping the device. Chemotactic migrated bacteria within a given time interval were collected for off-chip cultivation by pipetting. We introduced a parameter, called the chemotaxis index, to assess the chemotactic activity of bacterial cells.

Materials and methods

Bacterial strains and materials

The microbial species used are *Escherichia coli* (*E. coli*) RP437 carrying plasmid DsRedT.4 and *E. coli* RP1616 carrying plasmid pACGFP1 (Clontech Laboratories, Mountain View, CA). RP437 and RP1616 without exogenous plasmids were kindly provided by Professor J. S. Parkinson from the University of Utah.[32] RFP-tagged RP437 and GFP-tagged RP1616 were cultured overnight at 30 °C in a Luria-Bertani (LB) broth containing 100 μg mL^{-1} ampicillin. 20 μL overnight cultures were inoculated in 3 mL fresh LB broth and grew for 4 hours at 30 °C. Cells were collected by centrifugation at 6000 rpm for 3.5 min. The supernatant was discarded and the bacterial pellet was suspended in 1X PBS buffer containing 100 μM EDTA. The OD_{600} of the bacterial suspension was adjusted to 0.12 for the chemotaxis experiments unless otherwise stated. Solutions of aspartic acid (Asp) with a pH of 7.0 and nickel sulfate (Ni^{2+}) with a pH of 6.5 were prepared in 1X PBS as the attractant and the repellant, respectively.

Fabrication of the device

The optimized design of the device in AutoCAD 2006 format is provided in the ESI.† The device was fabricated using two glass plates by standard photolithography and wet chemical etching techniques.[33] The soda-lime glass plates coated with photoresist and chromium were ordered from Telic Company (Valencia, CA). Photomasks were design using AutoCAD (San Rafael, CA) and ordered from MicroCAD photomask Co. Ltd. (Shenzhen, China) The top plate contained microwells and ducts of 60 μm in depth and the bottom plate glass contained ducts of 20 μm in depth (Fig. 1B). The access holes on the top plate were drilled using a diamond drill bit 0.89 mm in diameter. The glass plates were thoroughly washed with ethanol, oxidized in a plasma cleaner (Harrick Plasma, Ithaca, NY), and silanized by 1*H*,1*H*,2*H*,2*H*-perfluorooctyltrichlorosilane (Fluorochem Ltd., Derbyshire, UK) in a vacuum desiccator for 4 hours. The glass plates were baked at 65 °C overnight, rinsed and dried again and kept in a clean Petri dish before use.

Device operation

The two plates of the device were assembled using about 3 μL of fluorinated oil (FC-40, 3M) which was added on the edge of the device, allowing the oil to wet the gap between the two glass plates by capillary force in about 10 min, to ensure smooth slipping and prevent leakage. Aqueous solutions of blue, red and yellow dyes were utilized to demonstrate the operation and diffusion process. First, different

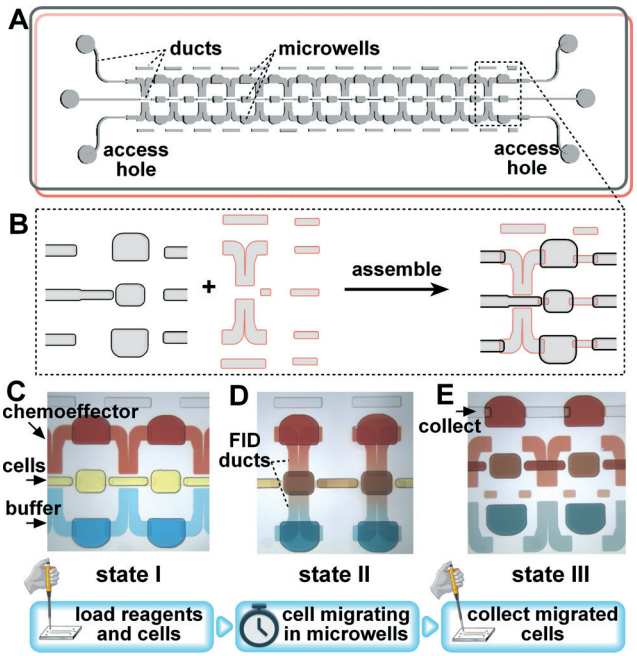

Fig. 1 The operation of the chemotaxis microfluidic device. (A) Schematic illustration of the device with multiple chemotaxis units. (B) Zoom-in view of the assembly of the top and the bottom plates; (C–E) step by step operation illustrated by food dyes. The device was loaded with CE (chemoeffector), BA (bacteria) and BF (buffer) at *state I*. After slipping, the loading ducts were disconnected from the microwells, which created a diffusion concentration gradient for bacterial chemotaxis at *state II*. Afterwards, the device was slipped again to terminate the experiment and collect the migrated cells.

solutions were injected into the three fluidic paths by pipetting (*state I*, Fig. 1C). Second, the top plate was slipped to the left, forming isolated units with three individual microwells connected by two ducts with effective lengths of 418 μm (*state II*, Fig. 1D). In each unit, the difference of concentration drove the diffusion between the microwells and a clear diffusion concentration gradient was formed across the ducts. After a certain time period, the top plate was slipped again (*state III*, Fig. 1E), disconnecting the 3 microwells in one unit and connecting the array of chemoeffector (or buffer) microwells with the short ducts for collecting the solutions by pipetting. Synchronized tests were conducted in all units simultaneously. After the experiment, the device could be opened, washed with detergent and ethanol, and reused repeatedly with virtually no limit.

Chemotaxis assays

The device was assembled as described above. A 10 mg mL^{-1} bovine serum albumin (BSA) solution was injected into all channels to treat the surface for 30 min prior to the assay to avoid cell adherence. After removing the BSA solution by applying vacuum *via* the access holes, the chemoeffector solutions were loaded to the top microwells, the bacterial suspension in PBS to the middle microwells and 1X PBS to the bottom microwells. Excess volume of the solutions was

injected for flushing out the residue of BSA in the microwells. The device was slipped to *state II*, during which the cells start to migrate freely from the center microwells to the ducts and microwells loaded with the chemoeffector or PBS. The device was placed on an inverted fluorescence microscope (Ti-Eclipse, Nikon, Japan) and the migration of the cells in the presence of the chemoeffector gradient was monitored with a timelapse of 5 min. Chemotaxis was evaluated by counting the number of cells in the chemoeffector microwells and PBS microwells at different time points. All the numbers provided are the average of five parallel units in one experiment. Finally, the device was slipped to *state III* and the migrated cells were collected for scale-up cultivation.

Numerical simulation

We used COMSOL Multiphysics (Stockholm, Sweden) to simulate the free interface diffusion process in the device. A diffusion coefficient of 4.9×10^{-10} m^2 s^{-1} was used for fluorescein, the model chemoeffector.[18]

Results and discussion

System design

Free interface diffusion (FID) based microfluidic devices can precisely control inter-diffusion between microwells connected by narrow ducts and were used for protein crystallization screening in small volumes.[34] Here, the dynamic diffusion concentration gradient based on FID together with the SlipChip technology was used for studying bacterial chemotaxis. As shown in Fig. 1, the designed device contained multiple FID chemotaxis units that were operated in parallel. The basic objective is to precisely control FID among three nanoliter microwells: a microwell (10 nL) to be loaded with bacterial cells in the middle and two microwells (16 nL) to be loaded with chemoeffector and 1X PBS buffer. First, we assembled the device (*state I*) and loaded individual solutions in their corresponding microwells. Then the device was slipped to *state II* and the three microwells were connected by the ducts. The concentration difference drove the formation of the chemoeffector gradient between the top microwell and the bottom microwell, resulting in the migration of bacteria from the middle microwells towards the top or bottom microwells according to their chemotactic preferences. The bacterial cells freely moved towards or against the FID gradient of the chemoeffector in the device with no shear stress. Because all three microwells are on the top plate with fixed distances and the duct is designed to be much longer and shallower than the microwells, with careful alignments, the FID gradient can be generated very reproducibly for the chemotaxis assays. By multiplexing the design, we can test multiple chemoeffectors or cell types (see the ESI† for an optimized design with 4 sets of assays). Furthermore, we can also enhance the device with different duct geometries and microwell volumes to introduce different gradient conditions in an array.

Characterization of the time-dependent diffusion process

To validate the FID process in the device, we used fluorescein as a model "chemoeffector". 100 μM fluorescein in 1X PBS was loaded into the upper channel and 1X PBS into the middle and bottom channels at *state I* and then the device was slipped to *state II* to form the experimental units (as shown in Fig. 1C and D), where the fluorescein started diffusing (Fig. 2). As shown in Fig. 2A, the numerical simulation revealed that a steep gradient in the duct towards fluorescein rapidly formed in less than 1 min. As the fluorescein quickly diffused into the middle microwell, a gradient inside the middle microwell also formed as early as 30 seconds, which means that the cells loaded in the middle microwells were exposed to the gradient of the chemoeffector at the very beginning. Spatial and temporal analysis showed that the gradients were mainly distributed in the ducts since they were much shallower than the microwells. The fluorescence reduced gradually in the chemoeffector microwells and increased in the middle and control microwells (Fig. 2C), showing a good agreement between the numerical and experimental data.

Since it took about 4–5 min to set up the multi-position imaging on the microscope, the timelapse fluorescence imaging was started at 5 min. As shown in Fig. 2B, linear gradients of the fluorescence intensity were observed in the

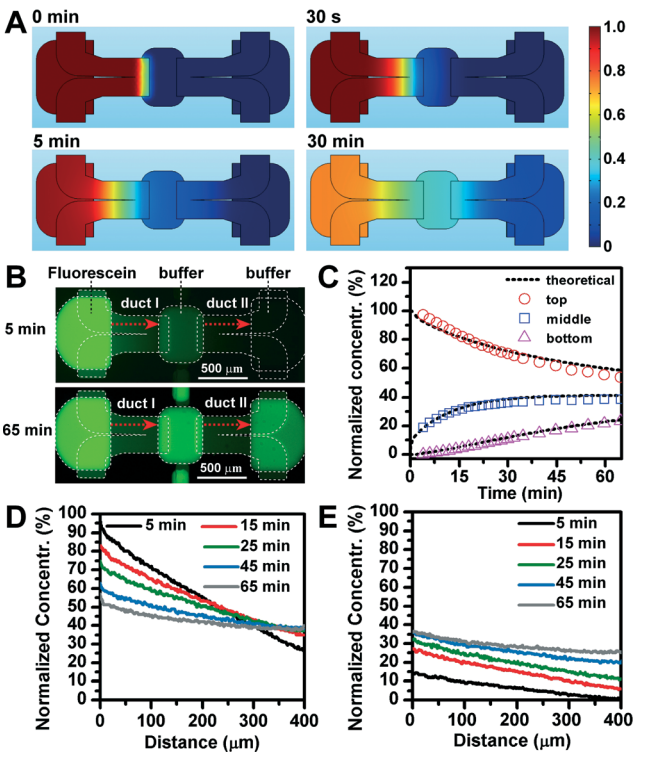

Fig. 2 The fluorescence intensity profiles. (A) Numerical simulation of free-interface diffusion of fluorescein and (B) fluorescence microphotographs at the beginning and 60 min later. The normalized fluorescence intensity profiles of the (C) three microwells in 60 min, and (D) duct I and (E) duct II at different time points.

ducts at 5 min after the ducts were connected to the microwells. We measured the fluorescence gradients in duct I and duct II as shown in Fig. 2D and E. The fluorescence intensities of the microwells and channels were normalized by subtracting the background signals and dividing the initial intensities. The diffusion experiments suggested that the concentration gradient could last longer than 1 hour, which is sufficient for the bacteria to make the chemotaxis choice. To provide a more stationary gradient, we could use microwells with bigger volumes for the chemoeffector and buffer on both sides and use shallower ducts to limit the diffusion speed.

Measurement of bacterial chemotaxis

It was noticed that time-dependent gradients in the ducts were not sufficient for absolutely quantitative chemotaxis assays since the concentration gradients were dynamically changing. Therefore, we evaluated the chemotaxis of the bacteria based on the number of migrated cells in the microwells containing the chemoeffector or the control buffer in a given time period. To test whether the microfluidic device was suitable for the reliable measurement of bacterial chemotaxis, we monitored the migration of RP437 over 1 hour with an interval of 5 min starting from 5 min after the slipping operation. We loaded cells (OD_{600} = 0.12) in the middle microwells, and tested the system with different chemoeffectors, including 200 μM Asp (attractant), 200 μM Ni^{2+} (repellent) and 1X PBS (control), filling the top microwells. As shown in Fig. 3, the attractant Asp, as well as the repellent Ni^{2+}, successfully induced obvious bacterial chemotactic responses. At 5 min, 10.3 cells migrated towards Asp with a standard deviation of 1.5 cells (expressed as 10.3 ± 1.5) and 1.8 ± 1.7 cells migrated towards the buffer. After 30 min migration, the average number of bacteria in the Asp microwells was 179 ± 11.7, while in the control microwells it was 2.8 ± 2.5, which showed an effective attraction of Asp on RP437 (Fig. 3B and C). A strong repelling effect of 200 μM Ni^{2+} on RP437 was also observed as shown in Fig. 3D, as the cells were swimming in the opposite direction. At 5 min, the cell number in the PBS buffer is 56.3 ± 4.0, compared to 0 in the microwells with Ni^{2+}. At 30 min, the cell number in the PBS buffer microwells is 152.2 ± 24.8, compared to 0.3 ± 2.6 in Ni^{2+}. A control experiment was carried out with the chemoeffector microwell and the control microwell both loaded with PBS buffer (Fig. 3E). As a consequence, we found that the cells in both microwells were increasing at a similar rate, suggesting that no artificial chemotaxis was taking place in the device. These results showed a good reproducibility in the cell migration in the beginning (5 min) and throughout the 60 min, indicating that the rapid formation of the FID gradient was sufficient to avoid random migration of the cells away from the middle microwells.

To assess the chemotactic ability of the bacterial cells with a chemoeffector at a certain concentration, we introduced a parameter called chemotaxis index, which is simply,

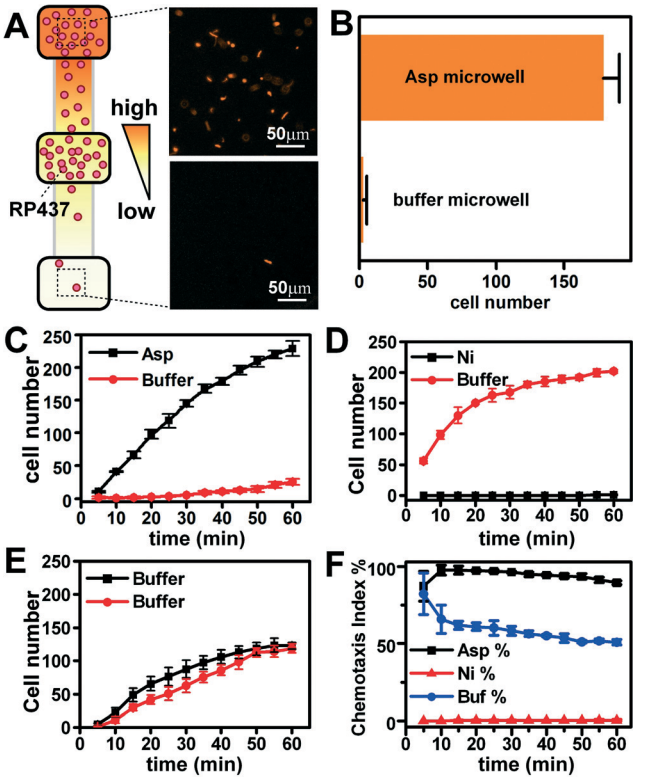

Fig. 3 The chemotaxis of *Escherichia coli* RP437 with different chemoeffectors on SlipChip. (A) Fluorescence microphotographs show RP437 to migrate into the microwells with Asp, 30 min after FID was initiated. (B) The statistics of the cell number in the effector and control microwells in panel A. (C–E) Continuous monitoring of *E. coli* RP437 migration with the chemoeffector microwell loaded with Asp, Ni^{2+} and 1X PBS buffer solutions. (F) The temporal tendency of the chemotaxis index for Asp, Ni^{2+} and 1X PBS (control).

$$I_t(\%) = \frac{N_e}{N_e + N_c} \times 100$$

where N_e and N_c are the number of cells that have migrated towards the chemoeffector and control microwells, and I_t is defined as the number of cells that have migrated towards the chemoeffector (N_e) divided by all cells migrated (N_e + N_c) in a given time period t. We didn't count the cells in the loading microwell because it also contained dead cells or cells with defects of the flagella or motility caused by sample preparation.

I_t is a percentage in between 0% and 100%, and can be used to indicate both positive and negative chemotaxes. In the beginning stage of diffusion, I_t cannot precisely reflect the chemotaxis response because it takes time for the cells to move through the 400 μm ducts and very few migrated cells into the chemoeffector and control microwells were observed. The optimal I_t and its t could be determined according to the diffusion coefficient of the chemoeffector and the motility of the bacterial cells. The value of I_t is approximately equal to 50%, if the cells do not respond to the chemoeffector. I_t increases to more than 50%, if the cells are attracted by the chemoeffector, and decrease to less than 50%, if the cells are repelled by the chemoeffector. Fig. 3F shows the curve of I_t as

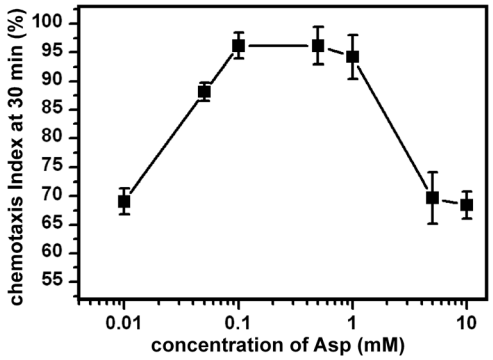

Fig. 4 The effect of Asp concentrations on chemotaxis of RP437 evaluated using the chemotaxis index at 30 min. Each point is the average result from 20 duplicated experiments.

a function of time for analyzing chemotaxis of RP437 towards Asp and Ni^{2+}. I_t of RP437 towards Asp is higher than 90% after 10 min and is around 0% for Ni^{2+}. In the control experiments, I_t stayed around 50%.

Based on the chemotaxis experiment analyses of RP437, we chose I_{30}, which is the chemotaxis index at 30 min, to evaluate the chemotaxis. Once I_{30} was defined as the evaluating parameter for the experiments, we set up multiple devices simultaneously without monitoring the process of migration, but waited for 30 min for each device, and slipped the devices from *state II* to *state III* under a stereoscope (as shown in Fig. 1E). The devices at *state III* can be stored at 4 °C if they are not going to be imaged immediately. The migrated cell numbers are counted to calculate I_{30} for all the devices. Therefore, the device is able to assess chemotaxis without relying on timelapse imaging, which is critical for other diffusion-based microfluidic devices for chemotaxis. Utilizing this procedure, the effect of Asp concentration in the range of 0 to 10 mM on chemotaxis of RP437 was studied. As shown in Fig. 4, RP437 had a strong response ($I_{30} > 80\%$) at Asp concentrations from 50 μM to 1 mM. When the concentration of Asp was decreased to 10 μM, I_{30} was 68%, indicating a decrease of efficiency. In general, I_{30} provided valuable information about the speed and intensity of chemotaxis for RP437, which helped us to evaluate how strong a chemotactic response was and what the optimal concentration range for the chemoeffector was.

Separation and collection of chemotactic bacteria

The device can selectively separate and enrich bacteria from a mixture based on motilities and chemotaxis responses of different species. This was tested using a 1 : 1 mixture of RP1616 (green) and RP437 (red) cells, as shown in Fig. 5. It has been noted that the strain RP1616 has poor motility and strain RP437 is highly motile towards Asp.[18] Before the test, both bacterial strains had similar cell numbers; the ratio of cells for the two strains was about 50%. After chemotaxis with Asp for 30 min, a significantly higher number of RP437 cells were detected in the chemoeffector microwells than RP1616, while in the control microwells, very few cells were collected. The analysis of the fluorescence microphotographs indicates that >96% of the cells were RP437 and <4% were RP1616 (Fig. 5C). Therefore, the two species were successfully separated.

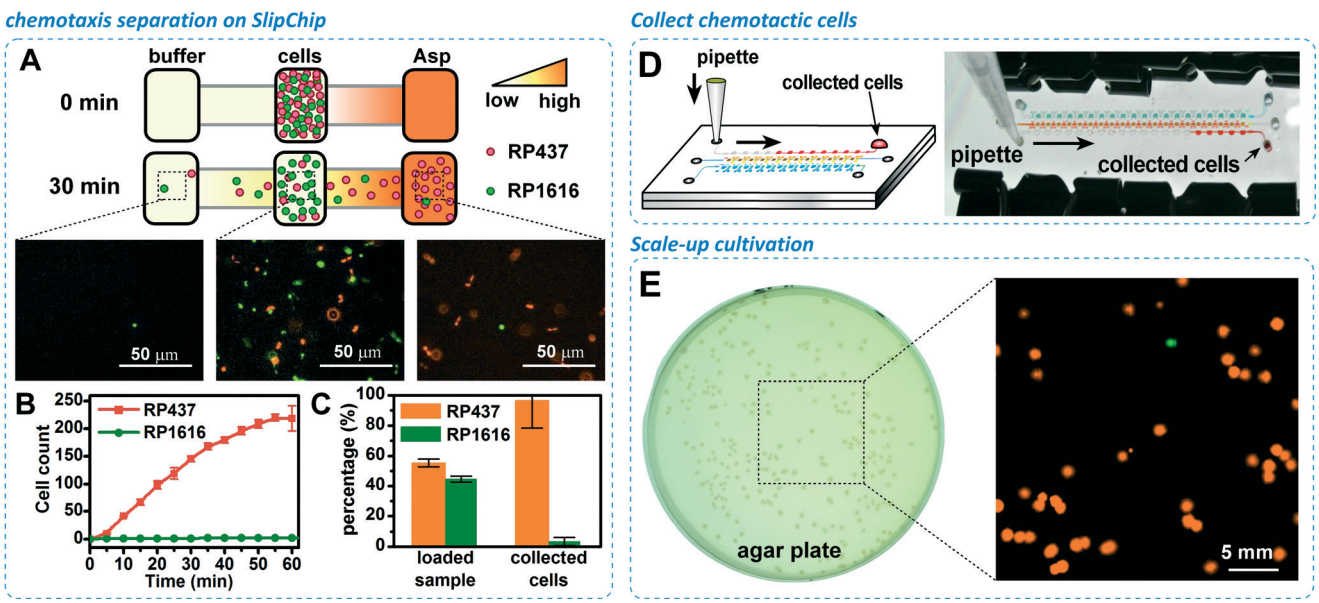

Fig. 5 Separation of chemotactic species from a mixture. (A) The schematic illustration represents the RP437 and RP1616 distribution on the device 30 min after FID started, with the loaded sample containing *E. coli* RP437 (red) and RP1616 (green) at a ratio of approximately 1 : 1; (B) the dynamic migration of RP437 and RP1616 with Asp as the chemoeffector over 1 hour; (C) the counted percentage of the two strains before and after 30 min chemotaxis; (D) the chemotactic bacteria were pipetted out of the microwells and collected; (E) the collected bacteria were plated on LB agar for cultivation. The green/red fluorescence overlay of the colonies grown from the single cells was obtained using an inverted microscope.

Furthermore, the chemotactic cells, which reached the chemoeffector microwells, can be easily collected from the device. As shown in Fig. 5D, after slipping from *state II* to *state III*, the chemoeffector microwells were connected with an array of horizontal ducts and access holes. The bacterial cells were collected by using a 10 μL pipette. The collected cells are spread onto an LB plate and cultivated overnight. We found that 97% of the colonies grown from the single cells showed red fluorescence and only 3% showed green fluorescence (Fig. 5E), which was consistent with data obtained from the cell counting on the device.

Conclusion

In this work, we developed a simple microfluidic device for chemotaxis assay and selective separation of chemotactic species. The reconfigurable device provides a versatile approach for generating an FID concentration gradient of the chemoeffector, evaluating bacteria behavior, and harvesting bacteria of interest. The device can be easily cleaned and reused without further modification. Compared to existing diffusion-based or flow-based chemotaxis devices, this device has the following advantages: i) it is easy to set up and can generate a controllable concentration gradient based on the geometry of the ducts and the microwells; ii) the length and width of the ducts can be optimized along with the motilities of the different cells and the diffusion coefficient of the different chemoeffectors; iii) using the slipping operation, we can initiate or terminate the chemotaxis experiment easily, an optimal chemotaxis time can be chosen based on experiments and the corresponding chemotaxis index can be utilized for quantifying chemotaxis phenomena; iv) it is feasible to test attractants and repellents simultaneously, or to investigate the antagonistic effect of both; v) chemotactic bacteria can be selectively isolated in separated microwells by a slip, resulting in the separation of bacteria from a mixture; vi) it enables us to easily harvest bacteria with chemotactic responses by pipetting; vii) very low cost and can be used in common laboratories with no limitation of reuse.

In summary, this device has the merits that it imposes zero shear stress on bacterial cells, performs multiple parallel experiments on-chip, requires no external controlling instruments, and generates reliable results. The current device is designed for bacterial chemotaxis assays and can possibly be extended for studying other cells, such as cancer cells or neutrophils. Collectively, the device developed in this work provides a versatile and function-oriented designing capacity, to meet the requirement of controllable chemotaxis studies, and a practical workflow for the enrichment of chemotactic cells for a variety of applications. The device may also be utilized for isolating bacterial species or subpopulations which have stronger chemotactic responses to a certain selected chemical, for directed selection and evolution.

Acknowledgements

This work was supported by: the National Natural Sciences Foundation of China (grants 21205134 and 31230003); the program of China Ocean Mineral Resources R & D Association (grant DY125-15-R-02); the National High Technology Research and Development Program of China (2012AA092103); the Fundamental Research Funds for the Central Universities, and the Research Funds of Renmin University of China (12XNLI04); the State key Laboratory of Microbial Resources, Institute of Microbiology, Chinese Academy of Sciences (grant SKLMR-20120604).

References

1 M. Baggiolini, *Nature*, 1998, **392**, 565–568.
2 F. Balkwill, *Nat. Rev. Cancer*, 2004, **4**, 540–550.
3 J. G. Cyster, *Science*, 1999, **286**, 2098–2102.
4 H. Kitano, *Science*, 2002, **295**, 1662–1664.
5 H. Kitano, *Nat. Rev. Genet.*, 2004, **5**, 826–837.
6 A. J. Ridley, M. A. Schwartz, K. Burridge, R. A. Firtel, M. H. Ginsberg, G. Borisy, J. T. Parsons and A. R. Horwitz, *Science*, 2003, **302**, 1704–1709.
7 P. Friedl and K. Wolf, *Nat. Rev. Cancer*, 2003, **3**, 362–374.
8 G. K. Hansson, *J. Thromb. Haemostasis*, 2009, **7**, 328–331.
9 M. S. Pittman, M. Goodwin and D. J. Kelly, *Microbiology*, 2001, **147**, 2493–2504.
10 R. E. Parales, J. L. Ditty and C. S. Harwood, *Appl. Environ. Microbiol.*, 2000, **66**, 4098–4104.
11 J. Melin and S. R. Quake, *Annu. Rev. Biophys. Biomol. Struct.*, 2007, **36**, 213–231.
12 H. N. Joensson and H. A. Svahn, *Angew. Chem., Int. Ed.*, 2012, **51**, 12176–12192.
13 M. Wu, S. Huang and G. Lee, *Lab Chip*, 2010, **10**, 939–956.
14 T. M. Keenan and A. Folch, *Lab Chip*, 2008, **8**, 34–57.
15 S. Kim, H. J. Kim and N. L. Jeon, *Integr. Biol.*, 2010, **2**, 584–603.
16 T. Ahmed, T. S. Shimizu and R. Stocker, *Integr. Biol.*, 2010, **2**, 604–629.
17 J. Wu, X. Wu and F. Lin, *Lab Chip*, 2013, **13**, 2484–2499.
18 G. Si, W. Yang, S. Bi, C. Luo and Q. Ouyang, *Lab Chip*, 2012, **12**, 1389–1394.
19 C. Beta and E. Bodenschatz, *Eur. J. Cell Biol.*, 2011, **90**, 811–816.
20 H. B. Mao, P. S. Cremer and M. D. Manson, *Proc. Natl. Acad. Sci. U. S. A.*, 2003, **100**, 5449–5454.
21 C. Beta, T. Fröhlich, H. U. Bödeker and E. Bodenschatz, *Lab Chip*, 2008, **8**, 1087–1096.
22 G. M. Walker, J. Q. Sai, A. Richmond, M. Stremler, C. Y. Chung and J. P. Wikswo, *Lab Chip*, 2005, **5**, 611–618.
23 J. P. Diao, L. Young, S. Kim, E. A. Fogarty, S. M. Heilman, P. Zhou, M. L. Shuler, M. M. Wu and M. P. DeLisa, *Lab Chip*, 2006, **6**, 381–388.
24 E. Choi, H. Chang, C. Y. Lim, T. Kim and J. Park, *Lab Chip*, 2012, **12**, 3968–3975.

25 T. Ahmed, T. S. Shimizu and R. Stocker, *Nano Lett.*, 2010, **10**, 3379–3385.
26 W. B. Du, L. Li, K. P. Nichols and R. F. Ismagilov, *Lab Chip*, 2009, **9**, 2286–2292.
27 Y. Song, Y. Zhang, P. E. Bernard, J. M. Reuben, N. T. Ueno, R. B. Arlinghaus, Y. Zu and L. Qin, *Nat. Commun.*, 2012, **3**, 1283.
28 H. Liu, X. Li and R. M. Crooks, *Anal. Chem.*, 2013, **85**, 4263–4267.
29 L. Li, W. B. Du and R. F. Ismagilov, *J. Am. Chem. Soc.*, 2010, **132**, 112–119.
30 F. Shen, W. B. Du, E. K. Davydova, M. A. Karymov, J. Pandey and R. F. Ismagilov, *Anal. Chem.*, 2010, **82**, 4606–4612.
31 F. Shen, B. Sun, J. E. Kreutz, E. K. Davydova, W. Du, P. L. Reddy, L. J. Joseph and R. F. Ismagilov, *J. Am. Chem. Soc.*, 2011, **133**, 17705–17712.
32 J. S. Parkinson, *J. Bacteriol.*, 1978, **135**, 45–53.
33 Q. H. He, S. Chen, Y. Su, Q. Fang and H. W. Chen, *Anal. Chim. Acta*, 2008, **628**, 1–8.
34 C. L. Hansen, E. Skordalakes, J. M. Berger and S. R. Quake, *Proc. Natl. Acad. Sci. U. S. A.*, 2002, **99**, 16531–16536.